Ultrafast Rydberg-Valence Interactions and Photodissociation Dynamics of Trimethylamine: A Time-Resolved XUV Photoelectron Spectroscopy Experiment

Contact *r.s.minns@soton.ac.uk*

D. J. Hughes, H. J. Thompson, R. S. Minns
University of Southampton
School of Chemistry, Highfield, SO17 1BJ

M. A. Parkes
University College London
Department of Chemistry, 20 Gordon St, WC1H 0AJ

R. T. Chapman, E. Springate, J. O. F. Thompson
Central Laser Facility
STFC Rutherford Appleton Labs, Didcot, OX11 0QX

P. Krüger, D. A. Horke
Radboud University
Institute for Molecules and Materials, 6525 AJ Nijmegen.

Introduction

Deep UV excitation of tertiary amines leads to the population of low-lying Rydberg states. The subsequent electronic state dynamics leads to internal conversion driving populations transfer to lower lying Rydberg states, *and*, coupling to dissociative valence electronic state that lead to dissociation. The electronic state dynamics have been studied using UV probes in time-resolved photoelectron spectroscopy measurements, giving detailed insights into the initial Rydberg state population.[1] Dissociation products have been separately studied using various time-resolved ion yield measurements[2-4] and through time-resolved X-ray diffraction.[5] Combining details of both the initial electronic state dynamics and product formation however remains challenging such that unified measurements that can monitor all aspects of the reaction are highly valuable.

Here, we report on time-resolved photoelectron spectroscopy measurements of the deep UV driven photodissociation dynamics of Trimethylamine (TMA), a prototypical tertiary amine. We utilize and extreme ultraviolet (XUV) probe that allows us to monitor all aspects of the reaction from initial excitation, through to reaction product formation.

Experimental Details

Time-resolved photoelectron spectra of TMA following excitation by 200 nm (6.1 eV) photons have been measured using an extreme ultraviolet (XUV) probe (~21.5 eV) generated by high harmonic generation.

The TMA molecular beam was derived from expansion of a 2% TMA mixture in He through a pulsed nozzle. The expansion was skimmed and crossed the pump and probe laser beams at the entrance to a time-of-flight electron spectrometer.

Experiments were performed with both parallel and perpendicular relative polarisations of the pump and probe pulses. In all case the probe polarization was kept parallel to the electron time of flight axis and the pump polarization was varied. Due to the strong alignment induced by the initial excitation of the $3p_z$ Rydberg state, the different polarization combinations allowed us to extract overlapping signals related to the initially populated $3p_z$ Rydberg state, and the subsequently populated $3p_{x/y}$ states.

The photoelectrons were detected and characterised by an electron time-of-flight spectrometer to which different lens voltages were applied to enhance the signal yield in specific regions of the photoelectron spectrum. Using a lens voltage of 110 V we increase the detection efficiency over the 2-5 eV binding energy range. A lens voltage of 80 V was subsequently used to measure binding energies between 8-15 eV. These lens settings do not change the energy calibration or temporal characteristics of the obtained spectra but did have a significant impact on the photoelectron detection efficiency as a function of photoelectron kinetic energy.

Results

In figure 1 we plot the photoelectron spectrum of the electronic ground state against the background subtracted spectrum obtained at a delay of 2.4 ps (figure 1A) and at 150 ps (figure 1B). At delays of a few picoseconds we observe enhanced photoelectron intensity at binding energies of approximately 2.5 eV, related to the Rydberg state population, and depletions at binding energies where there are signals related to the electronic ground state. At later times, the enhancement shifts from the low binding energy region associated with the Rydberg state population to higher binding energies associated with the dissociation products.

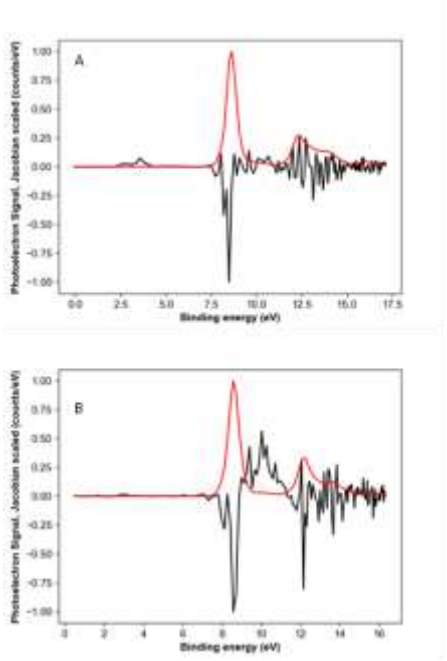

Figure 1. Background-subtracted photoelectron spectra of trimethylamine (black) and the pre-time-zero background (ground state) spectrum (red). (A) Spectrum at a pump-probe delay time of +2.4 ps, dominated by the ground state depletion signal in the binding energy ranges 8 – 16 eV and signals associated with the excited Rydberg states between 2 – 4 eV. (B) Spectrum at a pump-probe delay time of +150 ps. The ground state depletion is still clear but signals associated with photoproducts are seen between 9 – 12 eV.

In figure 2 we plot the time-resolved photoelectron spectrum over the binding energy range associated with the Rydberg state population. Initial excitation leads to population of the $3p_z$ Rydberg state, leading to the early time signal seen at a binding energy around 2.5 eV. Internal conversion through the $3p_{x/y}$ states lead to population trapping in the 3s Rydberg state and

signal appearing at a binding energy of 3.5 eV. The signal associated with the $3p_{x/y}$ is not clearly resolved in spectrum due to the effect of initial alignment upon excitation into the $3p_z$ state. Internal conversion to the perpendicularly aligned $3p_{x/y}$ states leads to a reduced ionization cross section while alignment is maintained.

The signal associated with the perpendicularly aligned $3p_{x/y}$ states can be seen using perpendicularly polarized pump and probe beams, as plotted in figure 3. Comparing figures 2 and 3 we see enhanced signal at binding energies close to 3 eV in the perpendicularly polarized configuration.

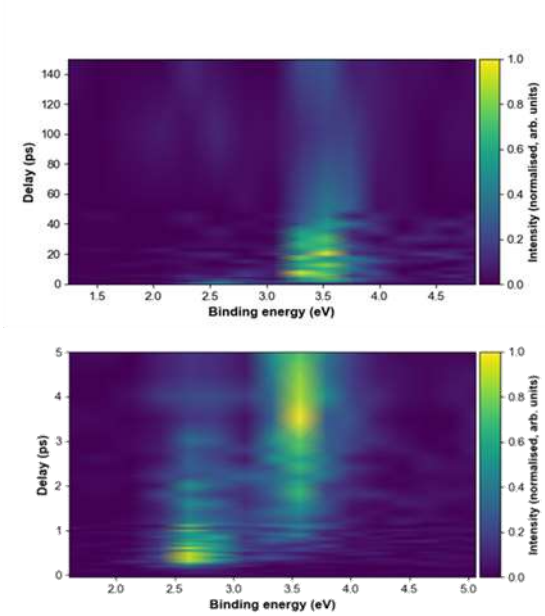

Figure 2. Time-resolved photoelectron spectrum of TMA. Signals measured over the pump-probe delay time ranges -0.05 - +5 ps (A), and -0.4 - +150 ps (B) with a parallel pump and probe polarisations.

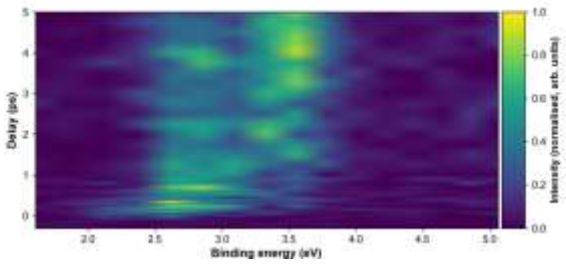

Figure 3. Time-resolved photoelectron spectrum of TMA measured with perpendicular pump and probe polarisations.

Due to the strong overlap between the various 3p Rydberg state component and the changing ionization propensity that will be depending on state population and alignment relative to the probe polarization we do not attempt to quantify the $3p_z$ and $3p_{x/y}$ states separately. This leads to a biexponential fit with time constants of 360 fs and 4.4 ps. The 4.4 ps decay correlates with the rising 3s signal. The 3s Rydberg state then decays with an exponential time constant of 70 ps. The assignment of the 360 fs time constant is still being explored but could relate to nuclear dynamics, the rotational dephasing time or, due to dissociation.

Turning our attention to the dissociation products seen in the photoelectron spectrum at higher binding energies, we plot the time dependence of the signals in figure 4. In figure 4 A we plot time integrated traces at three sperate delays to highlight the different timescales upon which the various products appear. The full time trace is plotted in figure 4 B, note the logarithmic time axis to highlight the products that form on very different timescales. The first products are seen on the few picoseconds timescale at binding energies above 10.3 eV. At longer delays products with binding energies between 9.3-10.3 eV are seen, rising over the next 100 ps. Analysis of the products is ongoing but initial assignments suggest that the products formed on the few picoseconds timescale are a vibrationally hot methyl (CH_3) in

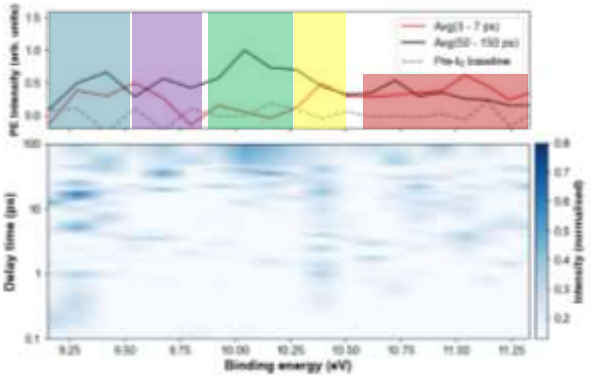

Figure 4. (A) Background-subtracted photoelectron spectrum concentrating on the product region (9 – 12 eV) averaged over the delay time ranges of 3 – 7 ps (red) and 50 – 150 ps (black) with a pre-time-zero baseline (grey dashed). We have highlighted 5 signal areas of interest in coloured boxes. (B) Time-resolved photoelectron spectrum of DMA plotted with a logarithmic time axis.

conjunction with ground state DMA ($\tilde{X}^2B_1$). The exponential rise see in these products approximately matches that associated with the decay of the 3p Rydberg states. The products appearing over the longer timescale, appear with a time constant that approximately matches that associated with the decay of the 3s Rydberg state and are assigned to vibrationally cold CH_3 and electronically excited DMA ($\tilde{A}^2A_1$) products.

We therefore suggest there are two dissociation processes, one that proceeds directly from the 3p Rydberg states and competes with internal conversion to the 3s Rydberg state, and one that proceeds via the 3s Rydberg state itself. The 4.4 ps time constant associated with the 3p Rydberg state, therefore appears to be controlled by both the internal conversion lifetime and the dissociation lifetime. With dissociation from the 3p Rydberg state leading to vibrationally excited CH_3 and ground state DMA. The CH_3 products obtained via the 3s Rydberg state are conversely vibrationally cold but appear with electronically excited DMA products.

Conclusions

We have measured the time-resolved photoelectron spectrum of TMA following 200 nm excitation. The measurements monitor the internal conversion process involved in the initial transfer of population among the 3p and 3s Rydberg states, as well as the eventual dissociation into fragments.

The measurements highlight two timescales of dissociation related to the 3p population with a time constant of approximately 4.4 ps, and the 3s state population with a time constant of approximately 70 ps. The fragments formed on these two timescales appear to have different levels of internal energy. Fragments formed directly from the 3p manifold are the ground electronic state of DMA in conjunction with vibrationally excited CH_3, while electronically excited DMA fragments are formed in conjunction with vibrationally cold CH_3 from the 3s state.

Acknowledgements

We thank the CLF for access to the Artemis facility. DJH thanks ELI beamlines and the School of Chemistry at the University of Southampton for a studentship. RSM thank the EPSRC for financial support (EP/R010609/1 and EP/X027635/1). DAH thanks the Netherlands Organization for Scientific Research (NWO) under grant number VIDI.193.037. DAH and PK thank the European Regional Development fund (EFRO, OP Oost) under project number PROJ-00949.

References

1. J. D. Cardoza, F. M. Rudakov, and P. M. Weber, *J. Phys. Chem. A*, 2008, **112**, 10736-10743.
2. N. R. Forde, M. L. Morton, S. L. Curry, S. J. Wrenn and L. J. Butler, *J. Phys. Chem.*, 1999, **111**, 4558- 4568.
3. N. R. Forde, L. J. Butler, B. Ruscic, O. Sorkhabi, F. Qi, and A. Suits, *J. Phys. Chem.*, 2000, **113**, 3088- 3097.
4. Y. Onitsuka, Y. Kadowaki, A. Tamakubo, K. Yamasaki, and H. Kohguchi, *Chem. Phys. Lett.*, 2019, **716**, 28-34.
5. J. M. Ruddock, N. Zotev, B. Stankus, H. Yong, D. Bellshaw, S. Boutet, T. J. Lane, M. Liang, S. Carbajo, W. Du, A. Kirrander, M. Minitti, and P. M. Weber, *Angew. Chem.*, *Int. Ed.,* 2019, **58**, 6371-6375.